# SUPPLEMENTAL INFORMATION

## Microwell Preparation

The desired microwell pattern was made on a silicon wafer using standard photolithography processes. In summary, a negative photoresist, SU-8 2035 (Microchem, Newton, MA, USA) was used for the master structure with a height of 50 μm. We prepared polydimethlysiloxane (PDMS, Sylgard 184, Dow Corning, Midland, MI, USA) with a base to curing agent ratio of 10:1. PDMS was cast on the master wafer and cured at 60˚C for 2 h. The microwell device was then assembled onto a commercially available glass slide and exposed to UV light for 30 min for sterilization. Each observation window unit consists of 2 hexadecimal digits, each of which is represented by 32 chambers (arranged in an 8×4 array) for alphanumerical representation, and the digits were patterned by 45˚-tilted square wells (**Fig. S2**).

## Cell Preparation

All cell lines used in this study were non-small cell lung cancer (NSCLC), including HCC827, H1650, and H1975, and purchased from the American Type Culture Collection (ATCC, Rockville, MD, USA), which authenticates tissues by their genotype. These cells were grown in either 25- or 75-$cm^2$ canted-neck flasks (Dow Corning, New York, USA). After reaching sufficient confluency of about 80%, cells were collected by trypsinization. All cells were cultured in Rosewell Park Memorial Institute (RPMI) Medium, which was supplemented with 10% fetal bovine serum (FBS; HyClone Laboratories Inc., Logan, Utah, USA), 1% sodium pyruvate (Gibco Invitrogen, Carlsbad, CA, USA) as an additional source of energy, and 1% Penicillin-streptomycin (Gibco Invitrogen, Carlsbad, CA, USA), using standard growth conditions of 37ºC and 5% $CO_2$. Cell cultures were regularly tested and verified free from mycoplasma infection.

## Sulforhodamine B (SRB) Cytotoxicity Assay

This protocol was adopted from the work by Vichai *et al*[1]. In summary, we have prepared a wide range of 2-fold serial dilutions (total of $2^{13}$, or 8,192-times dilution) of cytotoxicity reagents. A seeding density of $2 \times 10^4$ cells per well was maintained. After 3 h incubation in a 96-well array, HCC827 monolayers were fixed with 10% (wt/vol) trichloroacetic acid and stained with SRB for 30 min, followed by the removal of the excess SRB by washing three times with 1% (vol/vol) acetic acid. The protein-bound SRB was dissolved in 10-mM Tris base solution (pH 10.5) for optical density (OD) determination at 510 nm using a microplate reader (THERMO Max, Molecular Devices, Sunnyvale, CA, USA). The acquired OD results were analyzed by using the 4 Parameter Logistic (4-PL) nonlinear regression model, as in **Supplementary Fig. 3**.

## SUPPLEMENTARY FIGURES

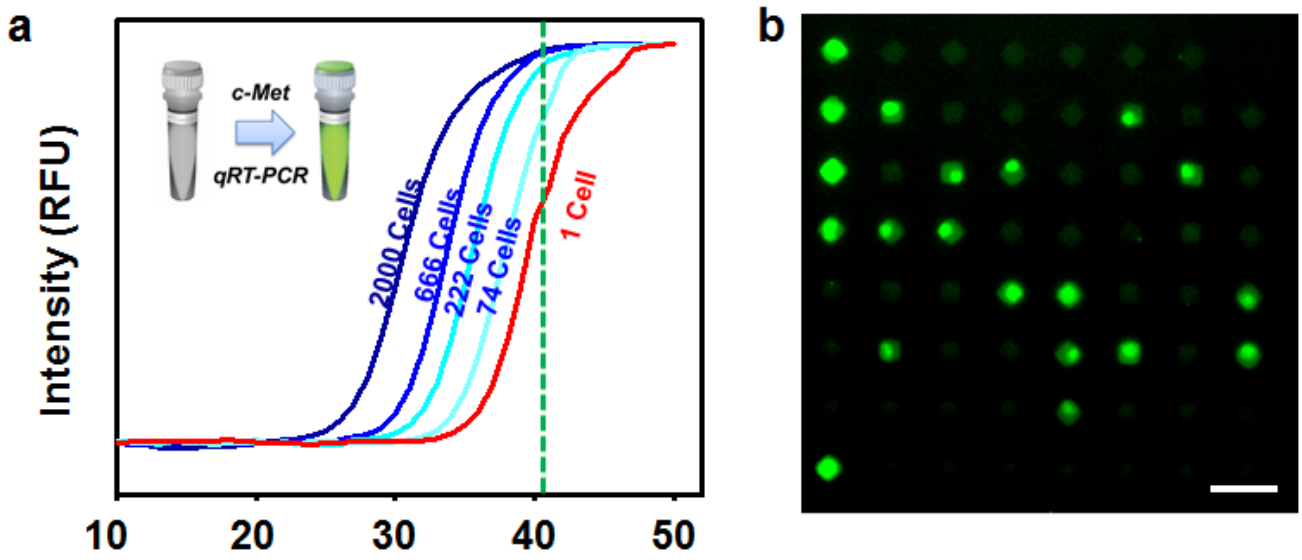


**Supplementary Figure 1.** (**a**) Optimization of PCR cycles for single-cell transcript amplification. 40 cycles were found ideal, where linear transcript expression response was expected according to the single cell's original amount of mRNA. (**b**) The representative micrograph of a unit of 64 wells after 40 cycles of PCR. Scale bar, 50 μm.

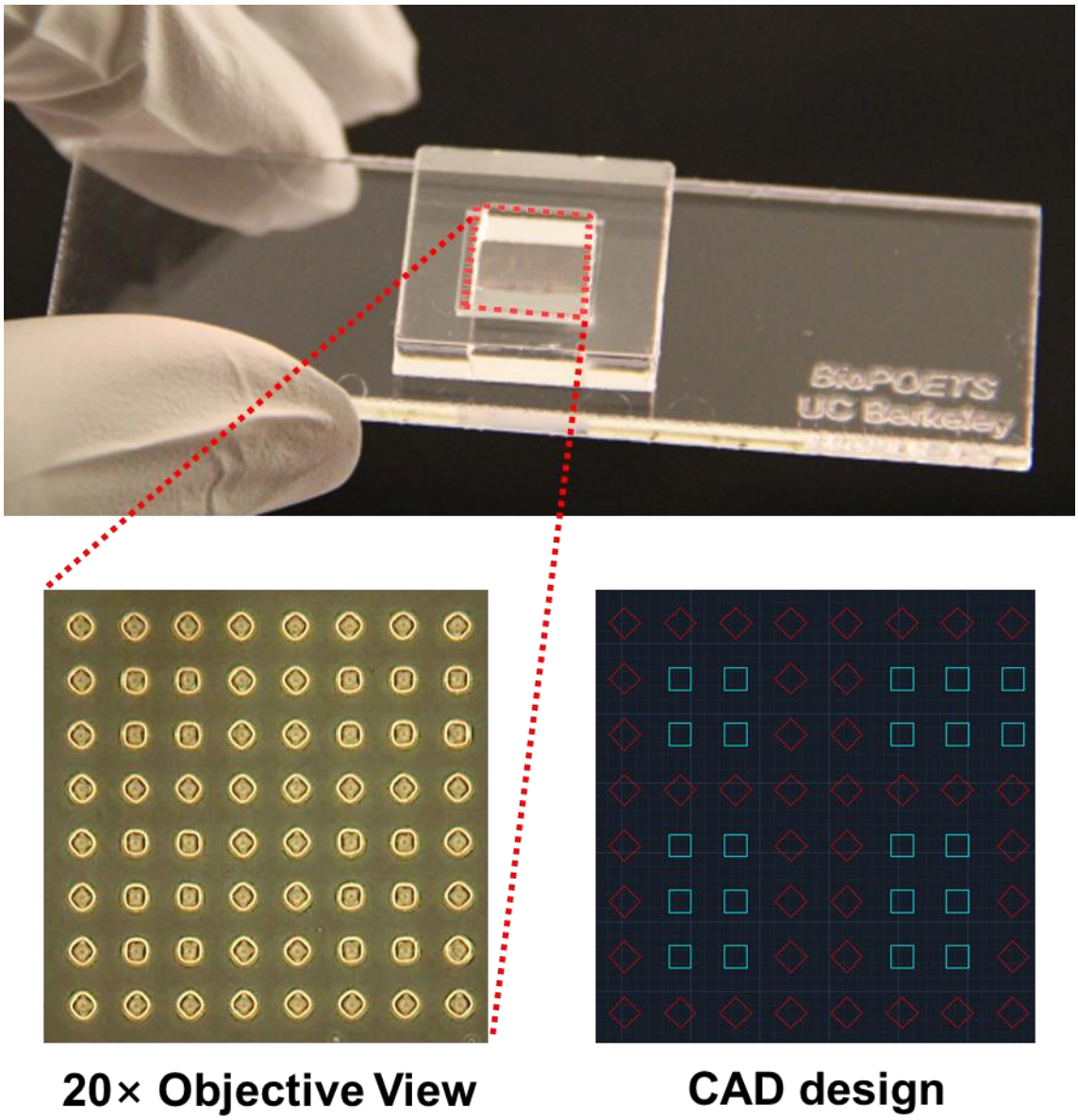


**Supplementary Figure 2.** A fabricated microfluidic device mounted on a commercially available glass slide. For liquid containment, a PDMS ring was placed on top. The expanded view shows a 64-well array encoded alphanumerically for identification. The corresponding AUTOCAD design is shown on the right.

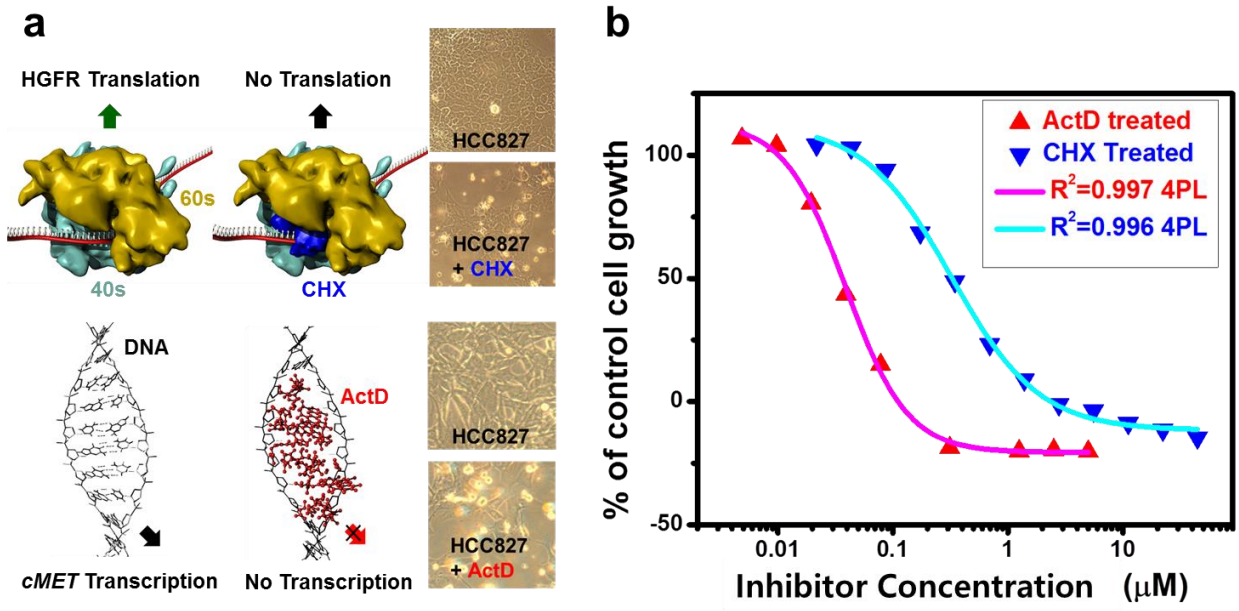


**Supplementary Figure 3.** (**a**) Top: Schematic diagram of the translational inhibitory mechanism of CHX and its effect on HCC827 after 1 d. Fifty percent of cells were eradicated due to the toxicity of CHX at $IC_{50}$. Bottom: Schematic diagram of the transcriptional inhibitory mechanism of ActD on HCC827 after 1 d. Fifty percent of cells were expunged due to the anti-cancer effect of ActD at $IC_{50}$. (**b**) A graphical representation of the cytotoxicity result obtained by SRB colorimetric assay. The graph shows the $IC_{50}$ values of CHX (325 nM) and ActD (40 nM) by fitting the result to the 4-parameter logistic nonlinear regression model. $IC_{50}$ values were used to find the appropriate dosages of CHX and ActD to HCC827 for device validation.

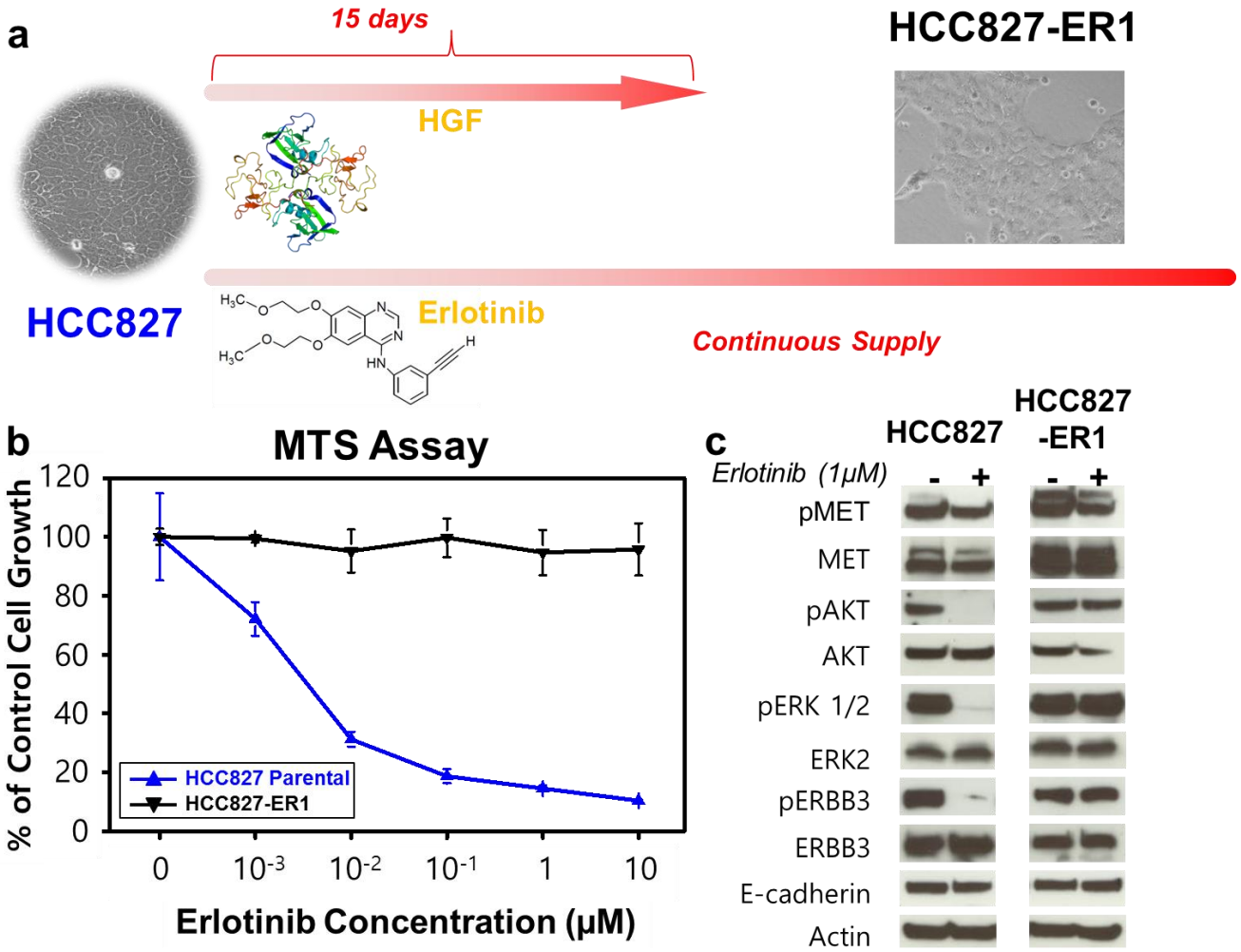


**Supplementary Figure 4.** (**a**) Schematic diagram for preparing HCC827-ER1. HCC827 cells were treated with HGF for 15 d and exposed to erlotinib continuously, resulting in a cell line resistant to erlotinib with an $IC_{50} \geq 5$ μM. (**b**) Graph showing percent of control cell growth over various erlotinib concentrations using MTS assay. While the percent of control cell growth significantly decreased for parental cell line with increasing erlotinib concentrations, HCC827-ER1 was unaffected. (**c**) The western blot analysis on lysed HCC827 and HCC827-ER1. Notably, concentration of cMET is higher in HCC827-ER1 than that of parental HCC827 cell line.

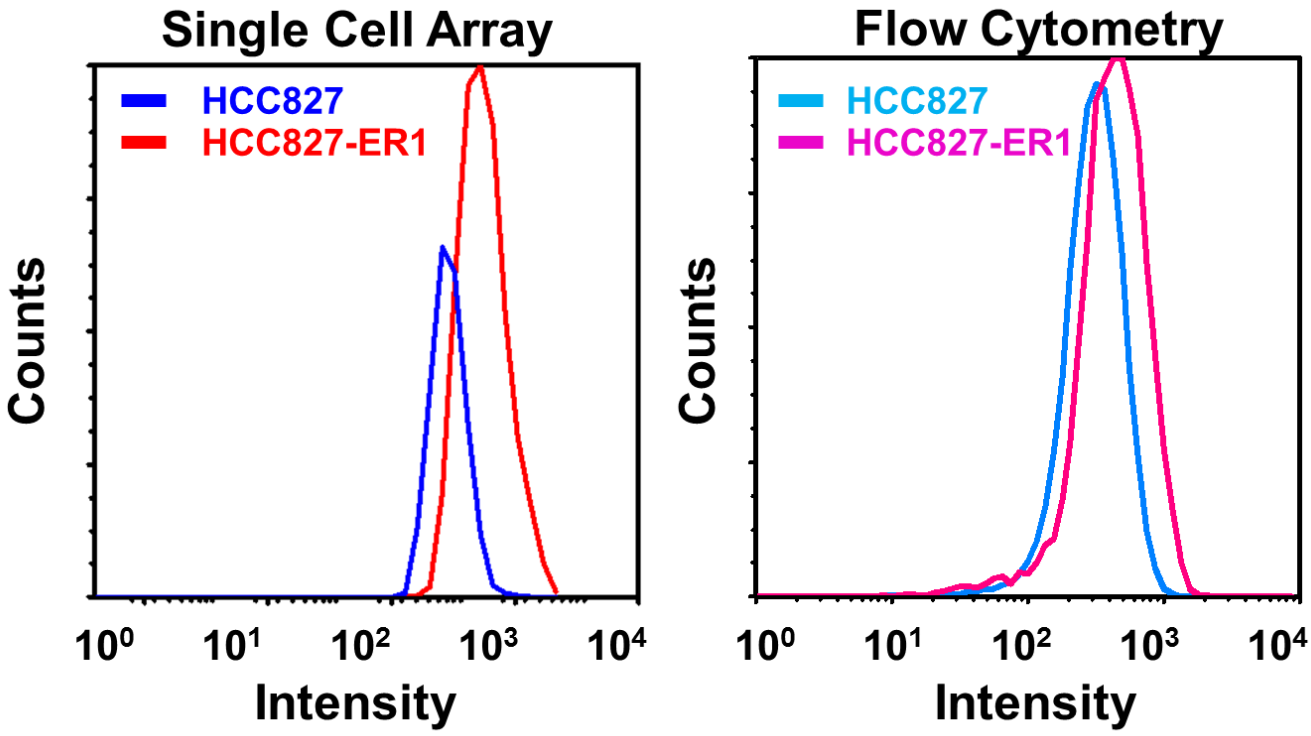


**Supplementary Figure 5.** The direct comparison of cMET abundance between single-cell array platform and flow cytometry data with the same cell lines. Normalizing the intensity of the single-cell array platform against flow cytometry data exhibited similar distributions, validating the single-cell array's reliability.

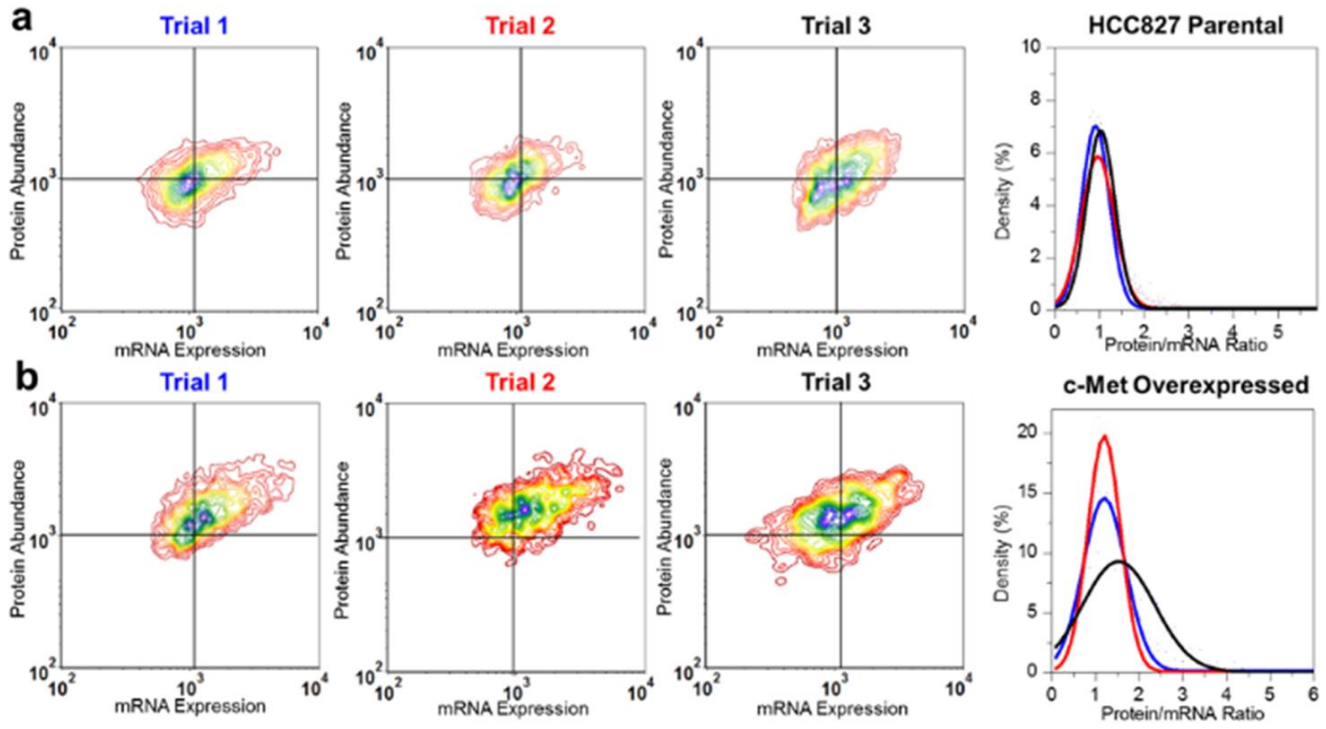


**Supplementary Figure 6.** mRNA – protein correlation experiments in triplicate. (**a**) Triplicate experiment on HCC827 parental cell lines. All trials show consistency in an mRNA/protein correlation pattern. The density plot of the single cell distribution according to its protein/mRNA ratio shows the expected overlap. (**b**) Triplicate experiment on HCC827-ER1. While all trials show consistency in a transcript-protein correlation pattern, the density plot of the single-cell distribution according to its protein-mRNA ratio shows the slight discrepancy due to loss of phenotypic responses from repeated passaging.

## Reference

1. Vichai, V. & Kirtikara, K. *Nat. Protoc.* **1**, 1112-1116 (2006).